THE JOURNAL OF BIOLOGICAL CHEMISTRY VOL. 288, NO. 26, pp. 18811–18824, June 28, 2013

Transcriptional Regulation by the Wilms Tumor Protein, Wt1, Suggests a Role of the Metalloproteinase Adamts16 in Murine Genitourinary Development*

Received for publication, February 25, 2013, and in revised form, May 8, 2013 Published, JBC Papers in Press, May 9, 2013, DOI 10.1074/jbc.M113.464644

Charlotte L. J. Jacobi[1], **Lucas J. Rudigier, Holger Scholz**[2], **and Karin M. Kirschner**

From the Institut für Vegetative Physiologie, Charité-Universitätsmedizin Berlin, Charitéplatz 1, D-10117 Berlin, Germany

Background: ADAMTS16 is a mammalian metalloproteinase with unknown function.
Results: Transcription of the *Adamts16* gene is regulated by Wilms tumor protein Wt1, and knockdown of Adamts16 reduces branching morphogenesis in cultured embryonic kidneys.
Conclusion: *Adamts16* is a Wt1 target gene during murine genitourinary development.
Significance: The findings provide novel insights into gene regulatory networks controlling kidney and gonad development.

ADAMTS16 (a disintegrin and metalloproteinase with thrombospondin motifs) is a secreted mammalian metalloproteinase with unknown function. We report here that murine Adamts16 is co-expressed with the Wilms tumor protein, Wt1, in the developing glomeruli of embryonic kidneys. *Adamts16* mRNA levels were significantly reduced upon transfection of embryonic murine kidney explants with *Wt1* antisense vivo-morpholinos. Antisense knockdown of *Adamts16* inhibited branching morphogenesis in kidney organ cultures. Adamts16 was detected by *in situ* mRNA hybridization and/or immunohistochemistry also in embryonic gonads and in spermatids and granulosa cells of adult testes and ovaries, respectively. Silencing of *Wt1* by transfection with antisense vivo-morpholinos significantly increased *Adamts16* mRNA in cultured embryonic XY gonads (11.5 and 12.5 days postconception), and reduced *Adamts16* transcripts in XX gonads (12.5 and 13.5 days postconception). Three predicted Wt1 consensus motifs could be identified in the promoter and the 5′-untranslated region of the murine *Adamts16* gene. Binding of Wt1 protein to these elements was verified by EMSA and ChIP. A firefly luciferase reporter gene under control of the *Adamts16* promoter was activated ~8-fold by transient co-transfection of human granulosa cells with a Wt1 expression construct. Gradual shortening of the 5′-flanking sequence successively reduced and eventually abrogated *Adamts16* promoter activation by Wt1. These findings demonstrate that Wt1 differentially regulates the *Adamts16* gene in XX and XY embryonic gonads. It is suggested that Adamts16 acts immediately downstream of Wt1 during murine urogenital development. We propose that Adamts16 is involved in branching morphogenesis of the kidneys in mice.

ADAMTS16 (a disintegrin and metalloproteinase with thrombospondin motifs) designates a growing family of secreted metalloproteinases in mammals and invertebrates (1, 2). Their structural and functional properties are related to, although distinct from, the ADAM[3] group of proteinases. ADAMTSs have several functional domains, including a pro-domain, an N-terminal catalytic domain, a disintegrin domain, and a C-terminal ancillary domain. The last one contains several thrombospondin-like repeats and is crucial for specific interactions with substrates (2, 3). ADAMTS proteins lack the transmembrane domain present in ADAMs (4). To date, 20 ADAMTS family members have been identified, whose multiple functions include proteolytic degradation of proteoglycans, collagen processing, inhibition of angiogenesis, and the control of blood coagulation (1, 2, 5–8). Additional roles of ADAMTS molecules may extend to embryonic development, inflammatory responses, and fertility (9–13). Mutations in *ADAMTS* genes can give rise to human disorders. For example, the Ehlers-Danlos syndrome type VIIC (MIM 2254109) is a recessive connective tissue disease, which results from mutations in the gene for the procollagen N-proteinase, ADAMTS2 (14). Mutations in the gene encoding ADAMTS13, which cleaves the von Willebrand factor, can lead to inherited thrombotic thrombocytopenia (15).

ADAMTS16 is a recently cloned family member, whose physiological functions are currently unknown. A full-length recombinant protein was capable of cleaving the proteinase inhibitor α_2-macroglobulin *in vitro* (16). *ADAMTS16* mRNA was initially detected in human fetal lung and kidney but also in adult brain and ovary (1). The cell types that express *ADAMTS16* in these tissues have not yet been identified. Later studies demonstrated *ADAMTS16* transcripts in human cartilage (17) and pancreas (16). Expression of ADAMTS16 in cartilage and synovium was increased in patients suffering from osteoarthritis compared with the tissues of healthy individuals (17). Variants of the *ADAMTS16* gene were recently linked to inherited arterial hypertension (18), and high levels of

* This work was supported in part by Deutsche Forschungsgemeinschaft Grant Scho634/8-1.
[1] Recipient of fellowships from the Sonnenfeld-Stiftung and the FAZIT-STIFTUNG.
[2] To whom correspondence should be addressed. Tel.: 49-30-450-528213; Fax: 49-30-450-528928; E-mail: holger.scholz@charite.de.

[3] The abbreviations used are: ADAM, a disintegrin and metalloproteinase; ADAMTS, a disintegrin and metalloproteinase with thrombospondin motifs; DIG, 3′-digoxigenin; ANOVA, analysis of variance; d.p.c., days postconception.

ADAMTS16 could be detected in a significant portion of esophageal squamous cell carcinomas (19).

Although a role of ADAMTS16 in development and disease is beginning to emerge, very little is known about the molecular mechanisms regulating its tissue-specific expression. *ADAMTS16* mRNA levels were increased in differentiated luteinizing human granulosa cells following treatment with follicle-stimulating hormone (FSH) and forskolin (16). These observations suggested that ADAMTS16 expression is activated via the cyclic AMP pathway (16). The promoter of the *ADAMTS16* gene is GC-rich and contains several consensus motifs for Egr1 and Sp1 (20). Both transcription factors were found to activate *ADAMTS16* promoter constructs in transient co-transfection experiments (20). However, it is not known whether Egr1 and Sp1 are physiological regulators of ADAMTS16 *in vivo*; nor have other *trans*-acting factors been ascertained thus far.

In view of this background, our study was aimed at providing novel insights into the gene regulatory mechanisms underlying the characteristic expression pattern of ADAMTS16. For this purpose, we analyzed the cellular distribution of Adamts16 protein in various organs of mice and rats. Furthermore, we sought to determine transcription factors that are involved in the tissue-specific control of *Adamts16*. We report here that *Adamts16* is a transcriptional downstream target gene of the Wilms tumor protein, Wt1. Importantly, knockdown of *Adamts16* by transfection with antisense vivo-morpholinos impaired branching morphogenesis in murine embryonic kidney cultures. These findings suggest a role for Adamts16 in the development of the genitourinary system in mice.

EXPERIMENTAL PROCEDURES

Plasmids—A 3250-base pair (bp) DNA sequence (from −3000 bp to +250 bp relative to the transcription start site) of the murine *Adamts16* gene (NCBI accession number NM_172053) was cloned by PCR, utilizing a bacterial artificial chromosome (imaGenes, Berlin, Germany, clone RPCIB731I01114Q) as template. The amplified product was ligated into the SacI and HindIII restriction sites of the pGL3basic reporter plasmid (Promega, Mannheim, Germany). *Adamts16* promoter constructs with gradually shortened sequences were generated by PCR. The PCR primers that were used for DNA amplification are listed in Table 1. All constructs were analyzed by automated DNA sequencing (Eurofins MWG, Ebersberg, Germany). The expression construct for the murine Wt1(−KTS) protein was kindly provided by Dr. Daniel Haber (Massachusetts General Hospital, Boston, MA).

Animals—A heterozygous ($Wt1^{+/-}$) mouse breeding pair (C57/BL6 (B6) strain) was obtained from the Jackson Laboratory (Bar Harbor, ME) and mated in the local animal facility in compliance with the current laws. The morning of vaginal plugs was considered as 0.5 days postconception (d.p.c.).

Cell Culture—COV434 human granulosa cells (catalog no. 07071909, HPACC) were maintained in DMEM nutrient (PAA Laboratories, Pasching, Austria) supplemented with 10% FCS (Biochrom KG, Berlin, Germany) and L-glutamine (PAA Laboratories). The UB27 and UD28 cell lines, which contain the murine Wt1(−KTS) and Wt1(+KTS) protein isoforms, respectively, regulated through a tetracycline-dependent promoter, were the gift of Dr. Christoph Englert. UB27 and UD28 cells and the murine mesonephros-derived M15 cell line (21) were cultured as described elsewhere (22, 23).

Organ Culture Experiments—Kidneys, gonads, and hearts were excised from embryos of timed pregnant mice (C57BL6 strain). The matched organs of each embryo were cultured separately on two polyethylene terephthalate Transwell® filters with 0.4-μm pore size (Corning, Inc.). This procedure allowed for a pairwise comparison between cultured explants from a single donor that had been transfected with either *Wt1* antisense or mismatch vivo-morpholinos (see below). The Transwell® filters were kept in DMEM nutrient with stable L-glutamine (PAA Laboratories) supplemented with 10% FCS (Biochrom KG), 100 IU/ml penicillin (PAA Laboratories), and 100 μg/ml streptomycin (PAA Laboratories) at 37 °C in a humidified atmosphere with 5% CO_2. Embryonic hearts were kept in 96-well plates for 5 days to allow outgrowth of epicardium-derived cells. The epicardial origin of outgrown cells was proven by their characteristic cobblestone-like appearance and robust expression of Wt1 (data not shown). Prior to morpholino treatment of the cells, the hearts were removed from the tissue culture plates. *In vitro* cultured organs and epicardial cell monolayers were incubated for 72 h with either *Wt1* antisense (CAGGTCCCGCACGTCGGAACCCAT) or mismatch (CAGCTCCGGCACCTCGCAACCGATG) vivo-morpholinos at 10 μM each (Gene Tools, Philomath, OR) (24). Whole cell lysates and total RNA were prepared from cultured organs and cells as described below. Sex determination of the embryos was performed by PCR amplification of the Y-chromosomal gene *Kdm5d* from DNA using the following primers: mKdm5d-F, CTGAAGCTTTTGGCTTTGAG; mKdm5d-R, CCACTGCCAAATTCTTTGG (25).

In order to study branching morphogenesis, the kidneys were isolated from mouse embryos at embryonic day 11.5 (Taylor stage 20) and cultured *in vitro* as described above. The organ rudiments were transfected either with *Adamts16* antisense (5′-CGCAGCACAACCTCGGGACTCCATG-3′) or mismatch vivo-morpholino (5′-CGGAGCAGAACGTCGGCACTCGATG-3′) at 10 μM each (Gene Tools) (24). After 72 h, the explants were formalin-fixed and double-stained with FITC-conjugated anti-pancytokeratin (diluted 1:100, Sigma-Aldrich) and anti-Wt1 antibody (C19, diluted 1:50, Santa Cruz Biotechnology, Santa Cruz, CA). Cy3-coupled donkey anti-rabbit IgG (diluted 1:100, Jackson ImmunoResearch, Hamburg, Germany) was used for the detection of bound Wt1 antibody. Photographs were taken, and branching of the pancytokeratin-stained ureter was analyzed using ImageJ software (National Institutes of Health, Bethesda, MD).

Cell Transfections and Reporter Gene Assays—COV434 cells were expanded to ~40% confluence in 24-well tissue culture plates. Firefly luciferase constructs, 200 ng each, harboring gradually shortened sequences of the murine *Adamts16* promoter and the 5′-UTR were transiently transfected along with a Wt1(−KTS) expression construct (200 ng) and a *Renilla* luciferase plasmid (100 ng), using the Fugene6® reagent (4 μl/well) as described in the supplier's manual (Roche Applied Science). As negative controls, transfections were performed with the

TABLE 1
PCR primers

Primer	Sequence
Cloning primers	
mAdamts16-Prom-3000	CGTGAGCTCAATTCAGACCTTTGCATA
mAdamts16-Prom-250	CGTAAGCTTCCGAGGGCTCACAGGACT
mAdamts16-Prom-1	GTAGAGCTCCCTTTGCCCTCCCTAGTCC
mAdamts16-Prom-45	ATAGAGCTCCACTGCCACTCCACCTCCC
mAdamts16-Prom-80	ATAGAGCTCCTGCCGGGTCGGTCCTTTG
qPCR primers	
mAdamts16-F	TTTCCACCAGAAGAGAACTG
mAdamts16-R	GGTGATCATCAGGACTTCG
hADAMTS16-F	TGGCTTTATTGTGCAGACG
hADAMTS16-R	GCCTCTTCTGTTCGTATCAT
mGapdh-F	ACGACCCCTTCATTGACCTCA
mGapdh-R	TTTGGCTCCACCCTTCAAGTG
hGAPDH-F	ACAGTCAGCCGCATCTTCTT
hGAPDH-R	GACAAGCTTCCCGTTCTCAG
ChIP primers	
mAdamts16-PromBS-F2	GTCATAGGCGTGAAGGATGC
mAdamts16-PromBS-R2	CCATGCACATCAGAGTTATC
mActin-ChIP-F1	ATAGGACTCCCTTCTATGAGC
mActin-ChIP-R1	TCCACTTAGACCTACTGTGCA
mAmhr2-PromBS-F1	CAGCTGGACAGCCAAGGTC
mAmhr2-PromBS-R1	CAGCCAAGGCTTCCTACAAA
hADAMTS16-Prom-BS-F5	TGCTCTTTGTCCCTGCACTCTC
hADAMTS16-Prom -BS-R1	CGCTCCGAGGGGCTAGGGGC
hACTIN-ChIP-F1	GTGAGTGGCCCGCTAACCT
hACTIN-ChIP-R1	CCTTGTCACACGAGCCAG

pGL3basic reporter plasmid (Promega) and the empty pCB6$^+$ expression vector, respectively. After 24 h, the transfected cells were lysed in Reporter Lysis Buffer (Promega), and luciferase activities were measured in a luminometer (Microlite TLX1, MGM Instruments, Hamden, CT) as described (26, 27). Data are presented as firefly luciferase activities normalized to *Renilla* luciferase activities.

Transfection of siRNA—M15 cells were grown to ~60% confluence in 6-well culture plates. A pool of four different siRNAs (50 pmol/well, Dharmacon, Thermo Fisher Scientific) targeting the murine *Wt1* gene (ON-TARGETplus, SMARTpool siRNA, L-040686-01-0005, NM_144783) were transfected using the DharmaFECT 1 reagent (Dharmacon) according to the manufacturer's protocol (22). Four different non-targeting siRNAs (siGENOME non-targeting siRNA pool 2, Dharmacon) were used as negative control. The cells were harvested for mRNA and protein analysis 2 days after siRNA transfection.

Reverse Transcription (RT) Real-time PCR—Total RNA was isolated from primary tissues and cells with the RNeasy Micro Kit (Qiagen, Hilden, Germany) and from permanent cell lines with the TRIzol LS reagent (Invitrogen). First-strand cDNA synthesis was carried out using oligo(dT) primers and SuperScript™ II reverse transcriptase (Invitrogen). Real-time PCR amplification was performed with the SYBR® Green PCR Master Mix and the StepOnePlus™ system (Invitrogen) as described in detail elsewhere (28). The PCR primers for real-time RT-PCR are listed in Table 1. Relative transcript levels were obtained by subtracting the threshold cycle (*Ct*) value of the housekeeping gene (β-actin or *Gapdh*) from the corresponding *Ct* value of the gene of interest. Differences in mRNA levels were calculated according to the expression $2^{\Delta\Delta Ct}$.

SDS-PAGE and Immunoblotting—Cells and tissues were lysed in Laemmli buffer (50 mM Tris-HCl, pH 6.8, 4 M urea, 1% (w/v) SDS, 0.001% (w/v) bromphenol blue, 7.5 mM DTT), disrupted by ultrasonication (Labsonic U, B. Braun, Melsungen, Germany), and subsequently heated to 95 °C for 5 min. Protein concentrations were measured spectrophotometrically according to the method of Warburg and Christian (29). Twenty μg of protein were loaded per lane and separated on a 10% denaturing polyacrylamide gel. The proteins were transferred onto a polyvinylidene difluoride membrane (GE Healthcare) with the use of a semidry blotting apparatus (Bio-Rad). Nonspecific binding activity was reduced by incubating the membrane for 60 min at room temperature in 5% nonfat milk (Roth, Karlsruhe, Germany) in TBS, 0.1% Tween 20. Incubation with Wt1 antibody (C19, catalog no. sc-192, diluted 1:400, Santa Cruz Biotechnology, Inc.) in 2.5% nonfat milk (Roth) in TBS/Tween was performed overnight at 4 °C. A polyclonal antibody raised in rabbit (diluted 1:5,000, ab45048, Abcam (Cambridge, UK)) was used for immunoblotting of Adamts16. After washing with TBS/Tween, the antibodies were detected with a peroxidase-coupled IgG (donkey anti-rabbit IgG-HRP, catalog no. sc-2313, diluted 1:20,000, Santa Cruz Biotechnology, Inc.), and the reaction products were visualized with Western Lightning™ Plus ECL reagents (PerkinElmer Life Sciences) following the user's manual. Equal protein loading was assessed with antibodies against actin (anti-actin clone C4, catalog no. MAB1501R, diluted 1:6,000, Millipore (Darmstadt, Germany)) and Gapdh (anti-Gapdh, catalog no. MAB374, diluted 1:300, Millipore), respectively, after stripping of the membranes with 1:5 diluted 1 N NaOH in distilled water for 10 min.

Electrophoretic Mobility Shift Assay (EMSA)—Non-radioactive EMSAs were performed with purified GST-tagged recombinant Wt1 proteins (30) and double-stranded oligonucleotides (Table 2), which were selected on the basis of predicted Wt1 binding sites in the promoter of the murine *Adamts16* gene. All oligonucleotides were 3′-digoxigenin (DIG)-labeled using the DIG Oligonucleotide 3′-End Labeling Kit (Roche Applied Sci-

TABLE 2
Oligonucleotides used for gel shift experiments (mutated nucleotides are underlined)

Oligonucleotide	Sequence
mAdamts16-wtA-sense	TCCTCTATCCCCTCCCCTCTCCTCTCCTTT
mAdamts16-wtA-antisense	AAAGGAGAGGAGAGGGGAGGGGATAGAGGA
mAdamts16-wtB-sense	GTGCTTTGCCGCCCCCCGCCACCACTGCCA
mAdamts16-wtB-antisense	TGGCAGTGGTGGCGGGGGGCGGCAAAGCAC
mAdamts16-wtC-sense	CTGCCACTCCACCTCCCGGTGCCGAACGAA
mAdamts16-wtC-antisense	TTCGTTCGGCACCGGGAGGTGGAGTGGCAG
mAdamts16-wtAmut-sense	TCCTCTATCGAATTCACTCTGCTCTCCTTT
mAdamts16-wtAmut-antisense	AAAGGAGAGTAGAGTGAATTCGATAGAGGA
mAdamts16-wtBmut-sense	GTGCTTTGAAGCTTCACGACATCACTGCCA
mAdamts16-wtBmut-antisense	TGGCAGTGATGTCGTGAAGCTTCAAAGCAC
mAdamts16-wtCmut-sense	CTGCCACTCAAGCTTCAGATGACGAACGAA
mAdamts16-wtCmut-antisense	TTCGTTCGTCATCTGAAGCTTGAGTGGCAG
mNtrk2-wt-F	TGTGAACTCCCACATGCTGCTG
mNtrk2-wt-R	CAGCAGCATGTGGGAGTTCACA

ence). Likewise, double-stranded oligonucleotides with mutations of the Wt1 binding motifs (Table 2) were DIG-labeled. For competition experiments, we used an oligonucleotide with a previously identified Wt1 binding site in the promoter of the *Ntrk2* gene (31). The binding reactions were carried out at room temperature for 1 h using 0.75 μg of recombinant Wt1 protein and 1 pmol of labeled oligonucleotide in 1× reaction buffer (10 mM Tris-HCl, pH 7.5, 50 mM KCl, 50 mM NaCl, 1 mM $MgCl_2$, 1 mM EDTA, 5 mM DTT, 5 mM phenylmethylsulfonyl fluoride, PMSF). DNA-bound proteins were separated on a non-denaturing 6% polyacrylamide gel and transferred with a semidry blotting system (Bio-Rad) on a positively charged nylon membrane (Roche Applied Science). After UV cross-linking (Stratalinker® UV cross-linker, Stratagene) and treatment with blocking reagent (Roche Applied Science), the membrane was incubated with anti-DIG-alkaline phosphatase antibody (catalog no. 11093274910, diluted 1:10.000, Roche Applied Science). Proteins were detected by nitro blue tetrazolium/5-bromo-4-chloro-3-indolyl phosphate staining (Roche Applied Science).

Chromatin Immunoprecipitation (ChIP) Assays—UB27 and UD28 cells were kept for 72 h in the presence or absence of tetracycline (1 μg/ml) to either inhibit or stimulate expression of Wt1(−KTS) and Wt1(+KTS) proteins, respectively. ChIP assays were performed with $\sim 4 \times 10^6$ cells. After fixation with 4% formaldehyde, the cells were disrupted by ultrasonication (Labsonic U, B. Braun) and centrifuged. The supernatants were diluted in immunoprecipitation buffer (0.01% SDS, 1.1% Triton X-100, 1.2 mM EDTA, 16.7 mM Tris-HCl, pH 8.1) and precleared for 1 h at 4 °C with DNA-blocked protein G-agarose (Millipore). The following antibodies and control sera were used (0.6 μg each) for overnight incubation at 4 °C: normal rabbit IgG (catalog no. sc-2027, Santa Cruz Biotechnology, Inc.), rabbit polyclonal anti-Wt1 antibody (catalog no. sc-192, Santa Cruz Biotechnology, Inc.). Immunoprecipitates were bound to DNA-blocked protein G-agarose (Millipore) during a 1-h incubation at 4 °C. Following several washing steps, the DNA was eluted in 1% SDS, 0.1 M $NaHCO_3$, extracted in 25:24:1 phenol/chloroform/isoamyl alcohol according to the supplier's instructions (Invitrogen), and subsequently precipitated in 100% ethanol. This protocol was also applied to M15 cells, which were used at $\sim 1 \times 10^6$ cells for ChIP assays. Immunoprecipitation with an anti-histone H3 antibody (catalog no. 07-690, Millipore) was performed as a control. Immunoprecipitated DNA was amplified by quantitative PCR using primer pairs that flanked the identified Wt1 binding sites in the murine *Adamts16* promoter (Table 1).

Immunohistochemistry—Immunofluorescent stainings were performed on mouse and rat tissues as described in detail elsewhere (26, 31). Briefly, embryos between 13.5 and 16.5 d.p.c. and tissues from adult animals were frozen in tissue-Tek O.C.T. compound (Sakura Finetek, Zoeterwoude, Netherlands) and sectioned using a cryostat. Frozen sections (8 μm) were treated with acetone/methanol (3:2) for 10 min at −20 °C and subsequently blocked for 5 min at room temperature in serum-free DakoCytomation protein block (catalog no. X0909, Dako, Hamburg, Germany). Single immunostainings for Wt1 and Adamts16 were performed on mouse tissue using the following primary antibodies diluted in ready-to-use antibody diluent (Zymed Laboratories Inc.. Berlin, Germany): Adamts16 rabbit (diluted 1:500, ab45048, Abcam), Adamts16 rabbit (diluted 1:50, catalog no. sc-50490, Santa Cruz Biotechnology, Inc.), anti-Wilms tumor protein Alexa Fluor® 488 (diluted 1:200, catalog no. ab140484, Abcam). Double immunostainings were performed on rat tissue using the above mentioned Adamst16 antibodies in combination with the Wt1 monoclonal mouse F6 antibody (diluted 1:600, catalog no. MAB4234, Millipore). For visualization of the bound primary antibodies, Cy3-AffiniPure donkey anti-rabbit IgG (catalog no. 711-165-152, diluted 1:200, Jackson ImmunoResearch) and Alexa Fluor® 488-AffiniPure donkey anti-mouse IgG (diluted 1:50, catalog no. 715-545-151, Jackson ImmunoResearch) were used. The cell nuclei were counterstained with 4′,6-diamidino-2-phenylindole (DAPI). Pictures of double stainings were taken with a digital camera connected to a confocal microscope (Leica DM 2500, Leica Microsystems, Wetzlar, Germany) utilizing LAS AF Lite software (Leica Microsystems). For pictures of single stainings, an epifluorescence microscope (Axiovert100, Carl Zeiss, Berlin, Germany) connected to a digital camera (Spot RT Slider, Diagnostic Instruments, Sterling Heights, MI) with the Spot software (Universal Imaging Corp., Marlow Buckinghamshire, UK) was used.

In Situ mRNA Hybridization—In situ hybridization for *Adamts16* mRNA was performed according to the protocol of Stricker *et al.* (32). Briefly, tissues were cryosectioned and fixed in freshly prepared paraformaldehyde (4% in PBS). Following acetylation with acetanhydride, the sections were prehybridized for 4 h at room temperature in hybridization buffer (5×

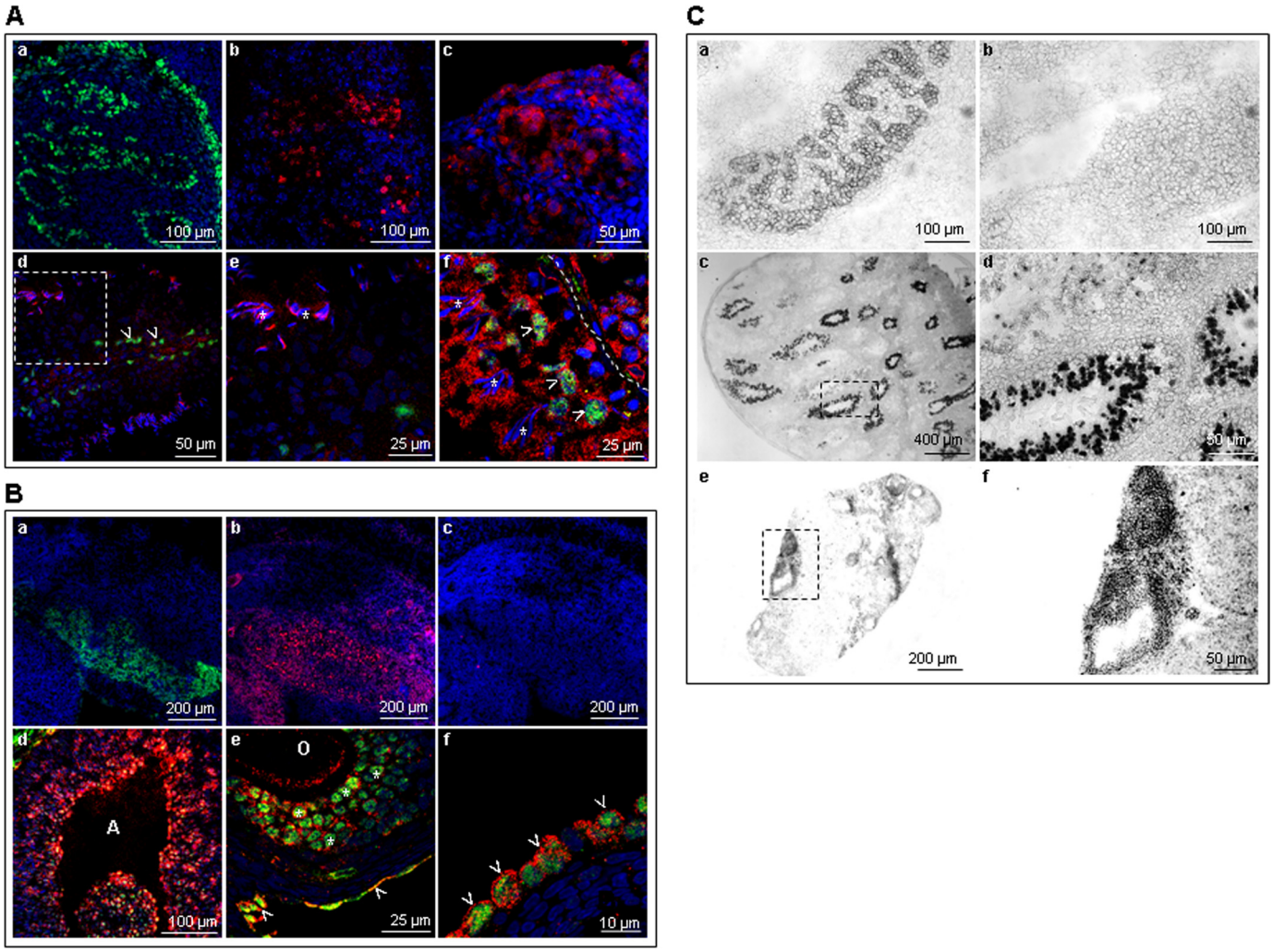

FIGURE 1. **Expression of Adamts16 and Wt1 in embryonic and adult gonads.** *A*, specific antibodies against Wt1 (*green*) and Adamts16 (*red*) were used to detect both proteins in the XY gonads of embryonic (14 d.p.c.) mice (*a–c*) and adult rats (*d–f*). Note that two different antibodies were applied for the detection of Adamts16; the results shown in *b*, *d*, and *e* were obtained with antibody ab45048 (Abcam), and antibody sc-50490 (Santa Cruz Biotechnology, Inc.) was used for the stainings presented in *c* and *f*. Double immunolabeling identified Sertoli cells as the sites of Wt1 expression in adult testes (*arrowheads* in *d* and *f*). Antibody ab45048 detected Adamts16 protein mainly in the spermatids (*asterisks* in *e*), whereas antibody sc-50490 produced a signal in Sertoli cells (*arrowheads* in *f*) in addition to spermatids (*asterisks* in *f*). Cell nuclei were counterstained with DAPI (*blue*). *B*, Wt1 (*green*) and Adamts16 (*red*) proteins in XX gonads of embryonic (13 d.p.c.) mice (*a* and *b*) and adult rats (*d–f*). Data shown in *b* were obtained with antibody ab45048 (Abcam), whereas antibody sc-50490 (Santa Cruz Biotechnology, Inc.) was used for the stainings presented in *d–f*. Co-expression of Wt1 and Adamts16 was observed in granulosa cells of preovulatory tertiary (*d*) and secondary (*asterisks* in *e*) follicles and in mesothelial cells on the surface of the ovaries (*arrowheads* in *e* and *f*). Incubation of the tissue sections with normal sera produced no staining signal (*c*). *O*, oocyte; *A*, antrum folliculi. Cell nuclei were counterstained with DAPI (*blue*). *C*, expression of Adamts16 in developing (*a*) and adult (*c* and *d*) testis was confirmed by *in situ* hybridization using a specific antisense riboprobe. Note that *Adamts16* transcripts were also present in granulosa cells of the ovaries (*e* and *f*). No hybridization signal was seen with the use of an *Adamts16 sense* probe (*b*). The data shown are representative for the five tissue samples from three different animals each.

SSC, 50% formamide). Hybridization was carried out overnight at 68 °C with digoxigenin-labeled murine *Adamts16* sense and antisense riboprobes, respectively. After washing with formamide (1× SSC, 50% formamide), the slides were treated with RNase for 30 min at 37 °C, and additional washing steps with SSC buffers (2× SSC, 0.2× SSC) were performed. The tissue sections were blocked for 1.5 h at room temperature (1% blocking solution in maleic acid buffer) and then incubated overnight at 4 °C with an alkaline phosphatase-conjugated anti-digoxigenin antibody. Bound antibody was visualized with nitro blue tetrazolium/5-bromo-4-chloro-3-indolyl phosphate reagent.

Statistics—Student's paired *t* test and ANOVA with Tukey's post hoc test were performed as indicated to reveal statistical significances. p values less than 0.05 were considered significant.

RESULTS

Adamts16 and Wt1 Proteins Are Expressed in Gonads and Kidneys—Although *Adamts16* mRNA has been detected by RT-PCR in several organs, including kidneys and gonads (1), very little is known about the protein localization in these tissues. We used specific polyclonal rabbit antibodies (ab45048 (Abcam) and sc-50490 (Santa Cruz Biotechnology, Inc.)) to visualize Adamts16-expressing cells in the genitourinary system of mice and rats. Adamts16 and Wt1 proteins were readily visible in XY and XX embryonic gonads (Fig. 1, *A* (*a–c*) and *B* (*a–c*)) although more distinct in embryonic testes (Fig. 1*A*,

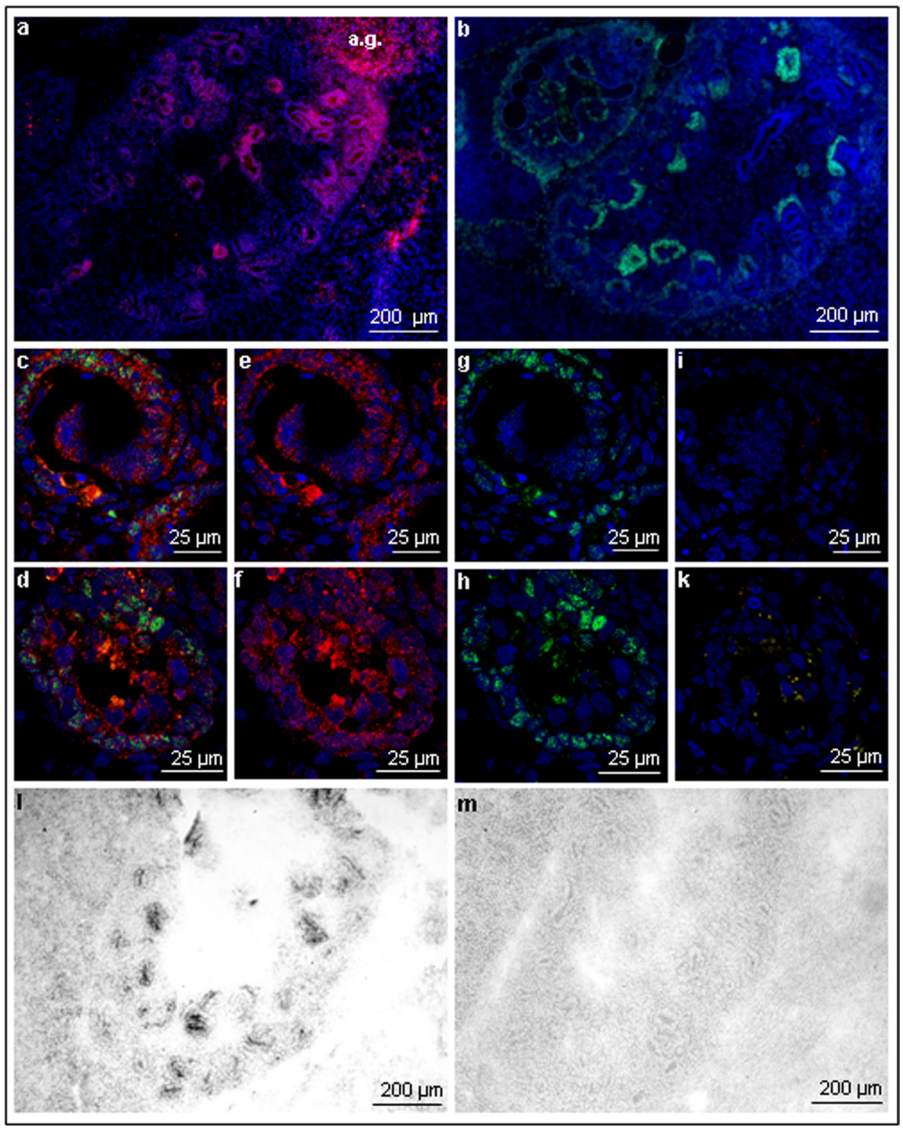

FIGURE 2. **Expression of Adamts16 and Wt1 in embryonic kidneys.** Specific antibodies against Wt1 (*green*) and Adamts16 (*red*) were used to detect both proteins in the kidneys of embryonic (16 d.p.c.) rats. Double immunofluorescent labeling indicates co-expression of Adamts16 and Wt1 in the developing glomeruli (*c* and *d*). The corresponding single stainings are shown in *e* and *g* and in *f* and *h*, respectively. Two different antibodies were applied for the detection of Adamts16: the results shown in *a*, *c*, and *e* were obtained with antibody ab45048 (Abcam), and antibody sc-50490 (Santa Cruz Biotechnology, Inc.) was used for the staining in *d* and *f*. Tissue sections were incubated with normal sera instead of primary antibodies as negative control (*i* and *k*). Cell nuclei were visualized with DAPI (*blue*). Note that the single immunostainings shown in *a* and *b* were performed on two different tissue sections. *Adamts16* mRNA was detected in the kidneys of murine embryos (14.5 d.p.c.) by *in situ* hybridization using a specific antisense riboprobe (*l*). No hybridization signal was obtained with the use of an *Adamts16 sense* probe (*m*). *a.g.*, adrenal gland.

a–*c*). According to previous reports (33, 34), Wt1 protein was present in developing and mature Sertoli cells (Fig. 1*A*, *a* and *d*–*f*), whereas immunhistochemistry (Fig. 1*A*, *b*–*f*) and *in situ* hybridization (Fig. 1*C*, *a*, *c*, and *d*) detected Adamts16 mainly in germ cells of embryonic and adult testes. Expression of Adamts16 was predominant in elongated spermatids of adult testes (Fig. 1*A*, *d*–*f*), which was confirmed by *in situ* hybridization (Fig. 1*C*, *c* and *d*). Both proteins were also detected in differentiated follicular granulosa cells and in mesothelial cells covering the surface of mature ovaries (Fig. 1*B*, *d*–*f*). *In situ* hybridization confirmed *Adamts16* transcripts in follicular granulosa cells of the ovaries (Fig. 1*C*, *e* and *f*). Adamts16 was demonstrated by immunostaining also in the developing glomeruli of embryonic kidneys (Fig. 2*a*), which are known sites of Wt1 expression (33, 34) (Fig. 2*b*). Co-expression of both proteins in glomerular progenitors was revealed by double immunolabeling with two different Adamts16 antibodies (Fig. 2, *c* and *d*, with corresponding single stainings in *e*–*h*). No fluorescence signal was obtained when normal sera instead of primary antibodies were used (Fig. 2, *i* and *k*). Adamts16 in murine embryonic kidneys (14 d.p.c.) was confirmed by *in situ* mRNA hybridization with a specific antisense riboprobe (Fig. 2*l*). No hybridization signal was obtained with the use of an *Adamts16 sense* probe (Fig. 2*m*).

Expression of Adamts16 in Developing Gonads and Kidneys Is Wt1-dependent—Co-expression of Adamts16 and Wt1 suggests a regulatory link between both proteins in different cell types of the genitourinary system. We therefore addressed the question of whether Wt1 is indeed necessary for normal expression of Adamts16 in embryonic gonads and kidneys. To

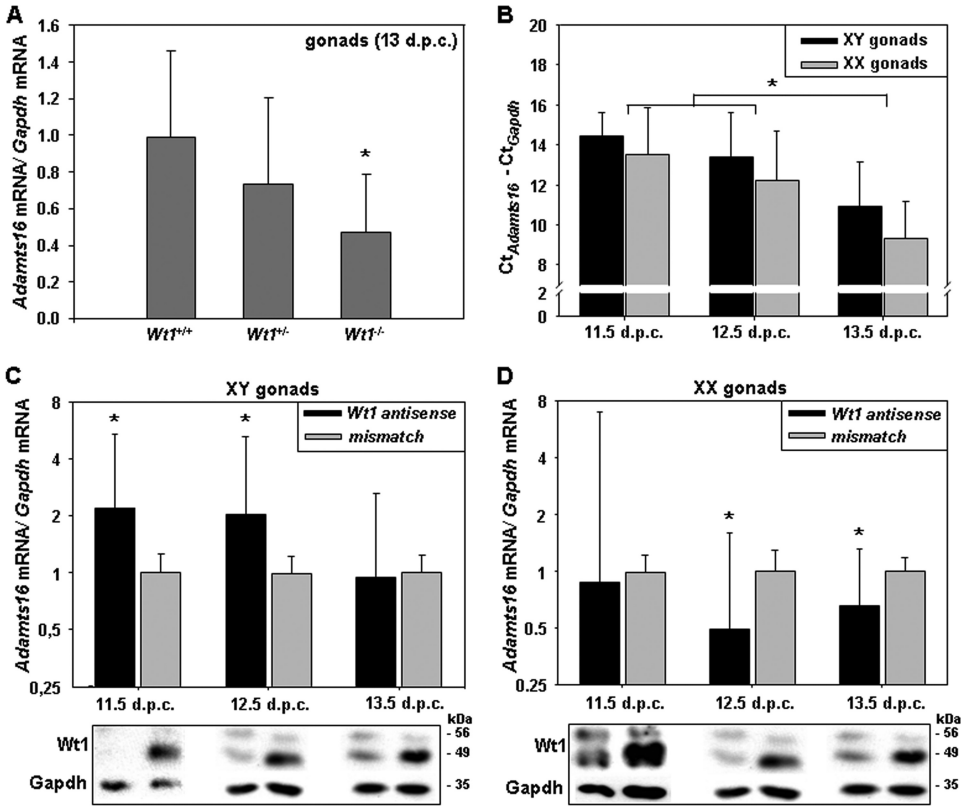

FIGURE 3. **Adamts16 mRNA in embryonic gonads.** *A*, *Adamts16* transcripts in freshly isolated gonadal ridges of wild-type ($Wt1^{+/+}$), heterozygous ($Wt1^{+/-}$), and *Wt1*-deficient ($Wt1^{-/-}$) murine embryos at 13 d.p.c. *Adamts16* mRNA levels were measured by quantitative RT-PCR and normalized to *Gapdh* transcripts. Values are means ± S.E. (*error bars*); $n = 9$ ($Wt1^{+/+}$), $n = 12$ ($Wt1^{+/-}$), $n = 14$ ($Wt1^{-/-}$); *, $p < 0.05$ *versus* wild type, ANOVA. *B*, *Adamts16* transcript levels in mismatch morpholino-treated (72 h) gonads presented as differences in *Ct* values ($Ct_{Adamts16} - Ct_{Gapdh}$). Assuming a doubling of amplicons during each cycle of the PCR, *Adamts16* mRNA levels were ~10 times higher in both XX and XY gonads at 13.5 d.p.c. *versus* 11.5 d.p.c. *C* and *D*, *Adamts16* mRNA in cultured gonads of wild-type male (*C*) and female (*D*) embryos at 11.5, 12.5, and 13.5 d.p.c. The isolated gonads were incubated for 72 h in the presence of either mismatch or *Wt1* antisense vivo-morpholinos. Results are shown as *x*-fold differences between cultures treated with mismatch and *Adamts16* antisense morpholinos, respectively. Wt1 and Gapdh proteins in the morpholino-treated tissues were determined by immunoblotting, and representative blots are shown. The expected molecular masses of the different Wt1 isoforms vary between 50 and 55 kDa (67). *Adamts16* and *Gapdh* transcripts were measured by RT-PCR. Data are presented as means ± S.E., $n = 12$. *, $p < 0.05$, Student's *t* test (*C* and *D*) and ANOVA (*B*).

this end, *Adamts16* transcripts were measured in isolated gonadal ridges of wild-type ($Wt1^{+/+}$), heterozygous ($Wt1^{+/-}$), and *Wt1*-deficient ($Wt1^{-/-}$) murine embryos at 13 d.p.c. Compared with the gonads of normal ($Wt1^{+/+}$) embryos, *Adamts16 mRNA* levels were significantly lower ($p < 0.05$, ANOVA) in the developing gonadal ridges of $Wt1^{-/-}$ mice (Fig. 3*A*). Later developmental stages could not be studied due to the embryonic lethality of *Wt1*-deficient mice (35). These observations suggest that *Adamts16* mRNA levels in the developing gonads depend, at least to some extent, on Wt1. However, it is also conceivable that reduced *Adamts16* transcripts were simply due to an arrest of gonad formation with subsequent apoptosis of the undifferentiated tissue in the absence of Wt1.

To distinguish between these possibilities, we established *in vitro* cultures of embryonic gonads. For this purpose, the gonads were excised from normal murine embryos at 11.5, 12.5, and 13.5 d.p.c., respectively, and grown in a culture medium supplemented with either *Wt1* antisense or mismatch vivo-morpholinos. After 72 h, total RNA was isolated from the explants, and *Adamts16* transcripts were measured by quantitative RT-PCR (Fig. 3, *B–D*). Down-regulation of Wt1 in response to *Wt1* antisense morpholino treatment, which was assessed by immunoblot analysis, had differential effects on *Adamts16* mRNA levels in female and male gonads (Fig. 3, *C* and *D*). Thus, *Adamts16* transcripts were significantly ($p < 0.05$, Student's paired *t* test) increased by knockdown of *Wt1* in XY gonads obtained from mouse embryos at 11.5 and 12.5 d.p.c. but not at 13.5 d.p.c. (Fig. 3*C*). In contrast, *Wt1* silencing significantly ($p < 0.05$, Student's paired *t* test) reduced *Adamts16* mRNA levels in XX gonads at 12.5 and 13.5 d.p.c. but had no significant effect on embryonic day 11.5 (Fig. 3*D*). These findings suggest that Wt1 inhibits *Adamts16* expression in XY gonads at early developmental stages (11.5 and 12.5 d.p.c.) and activates *Adamts16* expression in XX gonads at later points in time (12.5 and 13.5 d.p.c.). Consistently, *Adamts16* mRNA levels were increased in both XX and XY gonads treated with mismatch morpholinos, at 13.5 d.p.c. compared with earlier developmental stages ($p < 0.05$, ANOVA) (Fig. 3*B*). Based on differences in *Ct* values, *Adamts16* mRNA levels were at least 10-fold higher in male and female gonads from 13.5 d.p.c. *versus* 11.5 d.p.c. embryos (Fig. 3*B*). At all developmental stages analyzed, *Adamts16* transcripts were 2–3-fold higher in XX compared with XY gonads ($p < 0.05$, Student's paired *t* test) (Fig. 3*B*). Similar results were obtained when β-actin mRNA was used as a housekeeping gene for normalization (data not shown).

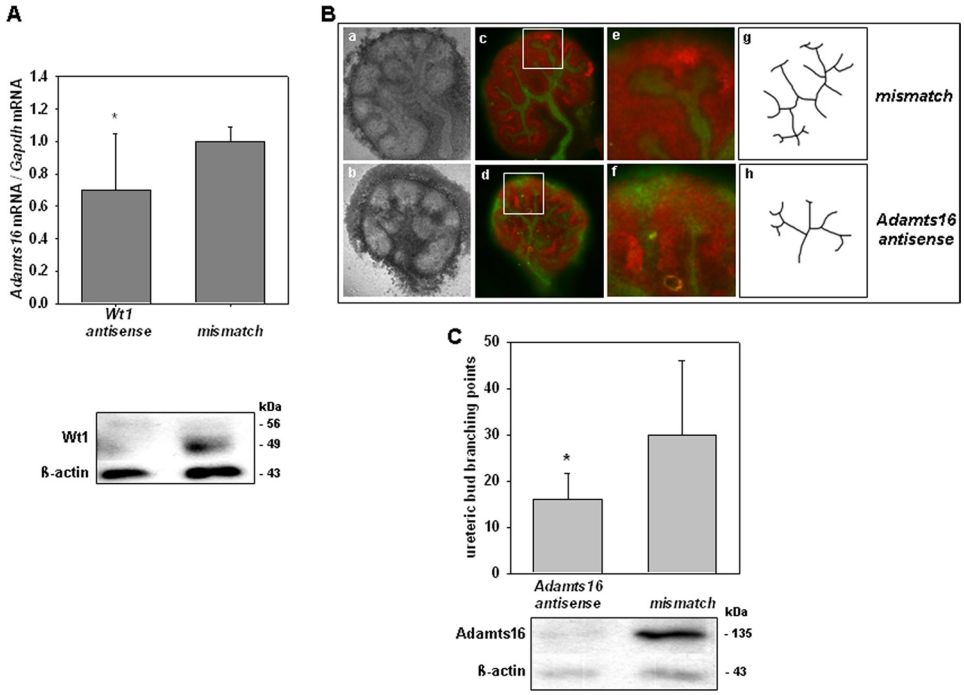

FIGURE 4. **Regulation and function of Adamt16 in embryonic murine kidneys.** *A*, *Adamts16* mRNA is reduced in kidney organ culture upon antisense inhibition of Wt1. Kidneys were removed from 13 d.p.c. murine embryos and incubated *in vitro* for 72 h with mismatch and *Wt1* antisense morpholinos, respectively. Knockdown efficiency was assessed by immunoblotting of Wt1 and β-actin proteins in the morpholino-treated cultures. A representative Western blot is shown in the *bottom panel* in *A*. *Adamts16* and *Gapdh* transcripts were measured by RT-PCR. Data are presented as means ± S.E. (*error bars*), $n = 7$; *, $p < 0.05$, Student's *t* test. *B*, *in vitro* differentiation of embryonic kidneys is impaired by antisense inhibition of Adamts16. Kidneys were isolated from murine embryos at embryonic day 11.5 (Taylor stage 20) and cultured for 72 h in the presence of either mismatch or *Adamts16* antisense morpholinos. The tissue explants were analyzed by phase-contrast microscopy (*a* and *b*) and immunofluorescent staining of the ureteric bud and the metanephric mesenchyme using antibodies against pancytokeratin (*green*) and Wt1 (*red*), respectively (*c–f*). Reconstructions of typical branching trees of the ureter are depicted in *g* and *h*. *C*, the number of branching points of the ureteric bud was significantly reduced in response to *Adamts16* knockdown. *Adamts16* knockdown in the kidney explants was assessed by immunoblot analysis, yielding a band of ~135 kDa (1, 19). A representative Western blot is shown in the *bottom panel* in *C*. Data are presented as means ± S.E., $n = 7$; *, $p < 0.02$, Student's paired *t* test.

Because $Wt1^{-/-}$ mouse embryos lack kidneys (35), they are not useful for analyzing Wt1 downstream signaling pathways during nephrogenesis. To overcome this problem, we established *in vitro* organ cultures of normal embryonic kidneys, in which we knocked down *Wt1* expression by antisense treatment (24). Densitometric analysis of the immunoblots using ImageJ software (National Institutes of Health) revealed a reduction of band intensities in response to *Wt1* antisense treatment by 57 ± 10% ($p < 0.05$, Student's paired *t* test, $n = 6$). Embryonic kidney explants treated with *Wt1* antisense vivo-morpholinos had significantly ($p < 0.05$, Student's paired *t* test) lower *Adamts16* mRNA levels than the corresponding mismatch controls (Fig. 4*A*). These findings indicate that normal expression of *Adamts16* in embryonic kidneys and gonads requires Wt1.

Knockdown of Adamts16 Inhibits Branching Morphogenesis in Kidney Organ Culture—To explore the potential role of Adamts16 in kidney development, we transfected embryonic renal organ cultures (Fig. 4*B*) with either *Adamts16* antisense or mismatch vivo-morpholinos. Knockdown efficiency was determined by immunoblot analysis of Adamts16 using the same antibody (ab45048, Abcam) as for the immunostainings. This antibody produced a signal of the predicted molecular mass (~135 kDa) of the Adamts16 protein (Fig. 4*C*). Importantly, the protein band was clearly diminished in kidney organ cultures that had been treated with antisense vivo-morpholinos against *Adamts16*, indicating specificity of the antibody used (Fig. 4*C*). *In vitro* knockdown of *Adamts16* resulted in an abnormal kidney morphology that was assessed by phase-contrast microscopy (Fig. 4*B*, *a* and *b*) and by immunostaining of the ureteric bud and the metanephric mesenchyme, respectively (Fig. 4*B*, *c–f*). Microscopic analysis of the immunolabeled whole-mount preparations revealed a significant ($p < 0.05$, Student's paired *t* test) reduction in the number of ureteric bud branching points upon *Adamts16* knockdown (Fig. 4, *B* (*g* and *h*) and *C*). These observations suggest a functional role of Adamts16 in branching morphogenesis of murine kidneys.

Wt1 and Adamts16 Expression Levels Are Correlated in Permanent Cell Lines and Primary Epicardial Cells—Next we examined whether Wt1 and *Adamts16* levels are associated in permanent cells derived from embryonic kidneys. M15 cells were originally established from the mesonephros of mice transgenically expressing the large T protein of polyoma virus under control of the early viral enhancer (21). The cells were transfected with a pool of four different siRNAs to inhibit Wt1 expression. Control experiments were performed by treatment with pooled non-targeting siRNAs. Silencing of Wt1 significantly ($p < 0.001$, Student's paired *t* test) reduced *Adamts16* mRNA levels in M15 cells, indicating that *Adamts16* expression in these cells depends on Wt1 (Fig. 5*A*). To analyze the expression of *Adamts16* and Wt1 in *primary* cells, we established cultures from epicardial progenitor cells. The epicardium is a

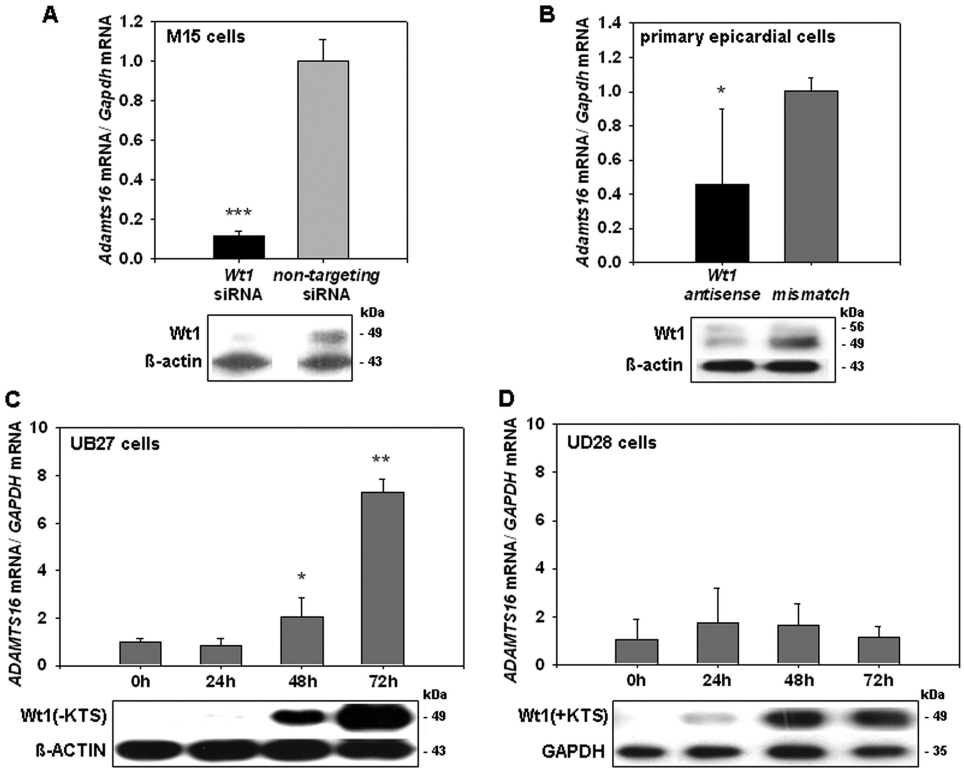

FIGURE 5. **Adamts16 transcripts and Wt1 protein in cell lines and primary epicardial cells.** *A*, *Adamts16* mRNA levels in murine mesonephros-derived M15 cells transfected with a pool of four different siRNAs targeting the *Wt1* gene. Control experiments were performed by incubation with non-targeting siRNAs. *B*, *Adamts16* transcripts in primary epicardial cells obtained from murine embryos. The cells were incubated either with *Wt1* antisense or mismatch vivo-morpholinos. *C* and *D*, *Adamts16* mRNA levels in UB27 (*C*) and UD28 (*D*) cells, which express the Wt1(−KTS) and Wt1(+KTS) isoforms, respectively, under control of a tetracycline-sensitive promoter. *Adamts16* and *Gapdh* transcripts were quantified by real-time RT-PCR. Values are shown as means ± S.E. (*error bars*); $n = 4$, M15 cells; $n = 4$, epicardial cells; $n = 3$, UB27/UD28 cells. Statistical significance is indicated by *asterisks* (***, $p < 0.001$; **, $p < 0.01$; *, $p < 0.05$, Student's *t* test). Wt1 protein was detected by immunoblotting (*bottom panels*) and compared with β-actin and Gapdh proteins, respectively. Representative Western blots are shown.

mesothelial tissue on the outer heart surface, which expresses Wt1 from the early developmental stages on throughout adulthood (34). We also detected Adamts16 protein by immunohistochemistry in the developing epicardium of murine embryos (data not shown). Transfection of primary epicardial cells with *Wt1* antisense vivo-morpholinos strongly reduced Wt1 protein levels, and this effect was associated with a significant ($p < 0.05$, Student's paired *t* test) reduction of *Adamts16* mRNA (Fig. 5*B*).

Importantly, the *Wt1* mRNA is subject to alternative splicing. The usage of an alternative splice donor site at the end of exon 9 leads to the insertion of an additional 3 amino acids, lysine, threonine, and serine (KTS), between zinc fingers 3 and 4 of the Wt1 protein (36). Structural and functional data demonstrate that Wt1(−KTS) proteins, which lack the 3 amino acids, act as transcription factors (37, 38). Compared with the Wt1(−KTS) isoforms, Wt1 proteins with the KTS insertion exhibit increased RNA binding affinity and play a presumed role in mRNA processing (39, 40). The human osteosarcoma-derived cell lines UB27 and UD28 express the Wt1(−KTS) and Wt1(+KTS) proteins, respectively, under control of a tetracycline-dependent promoter (23). A consistent rise of Wt1 proteins in UB27 and UD28 cells was achieved by removal of tetracycline from the tissue culture medium (Fig. 5, *C* and D). Induction of Wt1(−KTS) protein in UB27 cells resulted in a time-dependent increase of *ADAMTS16* mRNA levels (Fig. 5*C*), whereas accumulation of Wt1(+KTS) protein in UD28 cells had no significant effect on *ADAMTS16* transcripts (Fig. 5*D*). These results indicate that *Adamts16* is co-regulated with Wt1 in primary epicardial cells and permanent cell lines. Restriction of the stimulatory effect on *Adamts16* expression to the Wt1(−KTS) protein suggests that the underlying regulatory mechanism acts on the level of gene transcription.

Wt1 Protein Binds to the Promoter of the Adamts16 Gene in Vivo—ChIP was performed to examine whether Wt1 interacts with the promoter of the Adamts16 gene in M15 cells. The PCR primers for amplification of immunoprecipitated DNA bound to the proximal promoter and the 5′-flanking region of the *Adamts16* gene, respectively (Fig. 6*A*). Compared with the use of normal rabbit serum, *Adamts16* promoter DNA was enriched more than 2.5-fold with anti-Wt1 antibody ($p < 0.01$, Student's *t* test) (Fig. 6*B*). An ~2-fold enrichment of amplicons within the promoter of the *Amhr2* gene ($p < 0.05$, Student's *t* test), a known downstream target of Wt1 (41), was obtained by immunoprecipitation with anti-Wt1 antibody (Fig. 6*B*). In contrast, amplified DNA fragments containing an actin promoter sequence were not enriched by immunoprecipitation of Wt1 protein (Fig. 6*B*). These results could be validated using UB27 cells with inducible expression of the Wt1(−KTS) protein. Thus, *Adamts16* promoter DNA accumulated ~3-fold in UB27 cells with Wt1(−KTS) expression compared with uninduced cells ($p < 0.05$, Student's *t* test). No differences in Wt1-bound actin promoter DNA were observed between unstimulated and

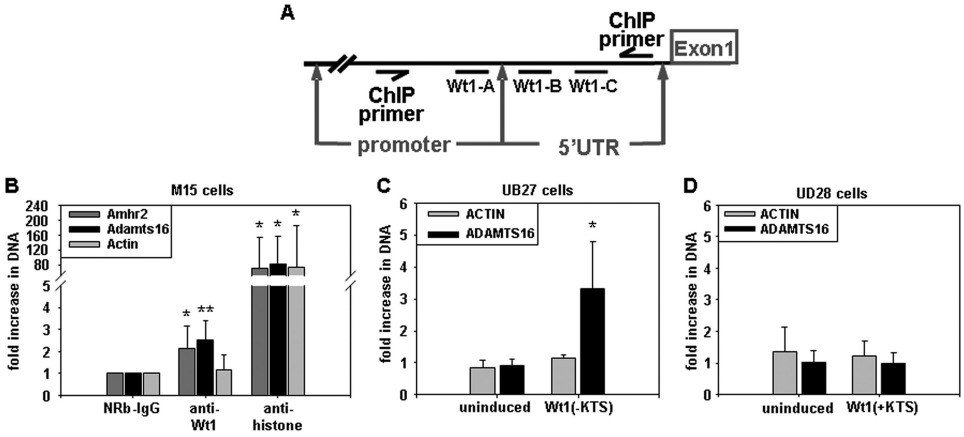

FIGURE 6. **Binding of Wt1 protein to the 5′-flanking region of the Adamts16 gene.** ChIP was performed to detect Wt1 protein bound to the 5′-flanking region of the *Adamts16* gene in its native chromosomal configuration. The drawing (*A*) delineates the three predicted Wt1 binding sites (*Wt1-A*, *Wt1-B*, and *Wt1-C*) in the promoter and 5′-UTR of the *Adamts16* gene and allocates the PCR primers used for DNA amplification. Specific antibodies against Wt1 and histone proteins were chosen for immunoprecipitation of M15 whole cell lysates. Amplicons encompassing the 5′-flanking region of the *Adamts16* gene were enriched ~2.5-fold with the use of anti-Wt1 antibody compared with normal rabbit IgG (NRb-IgG). No differences in actin DNA were observed between anti-Wt1 antibody and normal rabbit IgG (*B*). The gene encoding anti-Müllerian hormone receptor 2 (*Amhr2*), a previously identified Wt1 target (41), served as a positive control (*B*). Binding of Wt1(−KTS) protein to the *Adamts16* promoter was confirmed in stimulated UB27 cells (*C*). Wt1(+KTS) protein failed to interact with the promoter of the *Adamts16* gene in UD28 cells (*D*). Data shown are means ± S.E. (*error bars*). Statistical significances are indicated by *asterisks* (*, $p < 0.05$; **, $p < 0.01$, Student's *t* test; $n = 4$, M15 cells; $n = 3$, UB27/UD28 cells).

Wt1(−KTS) expressing UB27 cells (Fig. 6*C*). Immunoprecipitation with anti-Wt1 antibody failed to enrich *Adamts16* promoter DNA and actin DNA in UD28 cells that had been stimulated to express the Wt1(+KTS) protein (Fig. 6*D*).

The Wt1(−KTS) Isoform Stimulates the Adamts16 Promoter—To study the molecular interaction of Wt1 protein with the *Adamts16* promoter in detail, we co-transfected a firefly luciferase reporter construct, carrying ~3 kb of the upstream sequence of the murine *Adamts16* gene, and in addition a Wt1(−KTS) expression plasmid into human granulosa cells (COV434). A nearly 8-fold stimulation of the *Adamts16* promoter was measured in response to Wt1(−KTS) expression compared with co-transfection of the empty vector ($p < 0.01$, Student's *t* test) (Fig. 7*A*). Sequence analysis revealed the presence of three putative high affinity Wt1 binding sites in the promoter and 5′-flanking region of the murine *Adamts16* gene. All three elements were necessary for maximal activation of the *Adamts16* promoter by the Wt1(−KTS) protein (Fig. 7*A*). Truncated constructs with gradual deletion of the predicted binding motifs were successively less activated by co-transfection of the Wt1(−KTS) expression vector. Stimulation by the Wt1(−KTS) protein was completely lost in the absence of all three binding motifs (Fig. 7*A*). EMSAs verified that the Wt1(−KTS) protein indeed bound to each of these elements (Fig. 7, *B–D*). Interaction of recombinant Wt1(−KTS) protein could be competed with excess amounts of unlabeled oligonucleotide carrying the previously identified Wt1 binding site of the *Ntrk2* gene promoter (Fig. 7, *B–D*) (31). Likewise, binding of Wt1 protein was abrogated by introducing single base pair mutations into the three oligonucleotides (Fig. 7, *B–D*). These results demonstrate that Wt1(−KTS) protein interacts with several *cis*-elements in the 5′-upstream sequence and stimulates the promoter of the *Adamts16* gene. In contrast, recombinant Wt1(+KTS) protein did not interact with any of the identified binding sites (Fig. 7*E*).

DISCUSSION

ADAMTS16 is a mammalian metalloproteinase whose function is largely unknown. Our initial microarray gene expression analysis showed that *Adamts16* transcripts were strongly reduced upon RNAi silencing of the Wilms tumor protein Wt1 in mesonephros-derived M15 cells. The following chain of evidence suggests that *Adamts16* is indeed a molecular downstream target gene of the Wt1 transcription factor. First, *Wt1* and *Adamts16* mRNA levels were closely correlated in various tissues and cells (Figs. 3–5). Second, a reporter construct containing the murine 5′-upstream sequence of the *Adamts16* gene was stimulated ~8-fold by co-transfection of ovarian granulosa cells with a Wt1 expression vector (Fig. 7*A*). Moreover, Wt1(−KTS) protein bound to three presumed *cis*-elements in the promoter and the 5′-flanking region of the murine *Adamts16* gene (Figs. 6 and 7, *B-E*). Importantly, knockdown of *Wt1* in cultured embryonic murine kidneys and XX gonads (12.5 and 13.5 d.p.c.) by treatment with *Wt1* antisense morpholinos significantly reduced *Adamts16* transcripts, suggesting that Wt1 stimulates *Adamts16* expression in these tissues (Figs. 3 and 4*A*).

Transcriptional regulation of *Adamts16* by Wt1 may become relevant during various biological processes in the embryonic and adult organism. Thus, mammalian kidney formation depends on the reciprocal interaction between the metanephric mesenchyme and the invading ureteric bud (reviewed in Ref. 42). Signals emanating from the branching ureteric bud tips induce the surrounding mesenchymal cells to condensate and differentiate into comma- and s-shaped bodies, which eventually give rise to the glomeruli and build up parts of the tubular system of the kidneys (42). Epithelial transition of the metanephric mesenchyme in turn is a prerequisite for sustained branching of the ureteric bud tips during nephrogenesis (42). Metalloproteinases are considered as major candidates for the modulation of mesenchymal-epithelial interactions in embry-

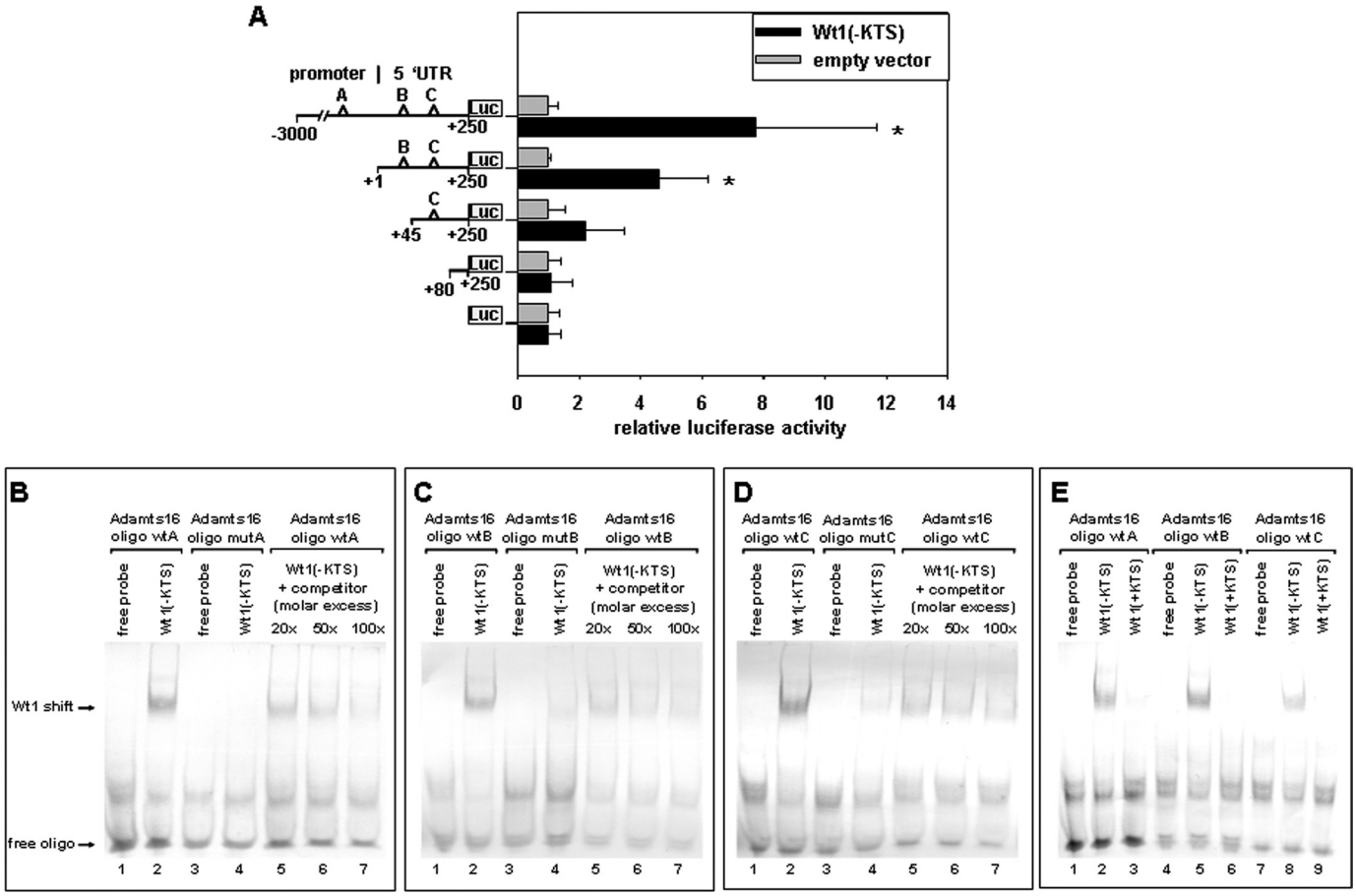

FIGURE 7. **Functional interaction of Wt1(−KTS) protein with the promoter of the *Adamts16* gene.** *A*, COV434 ovarian granulosa cells were transiently co-transfected with the indicated *Adamts16* promoter luciferase reporter plasmids and a Wt1(−KTS) expression construct. A *Renilla* luciferase plasmid was utilized for normalization of transfection efficiencies. Data shown are means ± S.E. (*error bars*), $n = 4$. Statistical significance *versus* transfection with empty expression vector is indicated by *asterisks* (*, $p < 0.05$, ANOVA). *B–D*, binding of Wt1(−KTS) to each one of the predicted binding sites (*lanes 1* and *2*) was proven by an electrophoretic mobility shift assay. Mutation of the Wt1 consensus motifs abrogated Wt1(−KTS) binding (*lanes 3* and *4*). Interaction of Wt1(−KTS) protein with the wild-type oligonucleotides could be competed with unlabeled competitor DNA (*lanes 5–7*) corresponding to the previously identified Wt1 binding element in the *Ntrk2* promoter (31). *E*, the Wt1(+KTS) isoform, which lacks 3 amino acids in its zinc finger domain (36), did not bind to the oligonucleotides (*lanes 3*, *6*, and *9*).

onic kidneys and other tissues. Several matrix metalloproteinases and their inhibitors (*i.e.* MMP-2, MT1-MMP, and TIMP-2) are spatially and temporally regulated in the developing kidney (43). Moreover, targeted inactivation of the gene encoding ADAMTS1, which cleaves the major cartilage proteoglycan aggrecan, produced kidney abnormalities in mice (*i.e.* shrinkage of the renal parenchyma and enlargement of the caliceal space) (44). Our observation that vivo-morpholino knockdown of *Adamts16* impaired branching morphogenesis in cultured murine embryonic kidneys suggests an involvement of this metalloproteinase in nephrogenesis (Fig. 4, *B* and *C*). Consistently, silencing of the nephrogenic Wt1 protein significantly reduced *Adamts16* expression in kidney rudiments (Fig. 4*A*). Wt1 belongs to the Cys_2-His_2 class of zinc finger proteins and promotes mesenchymal-to-epithelial transition during the early stages of kidney development (35, 45). Kidney formation in Wt1-deficient mouse embryos, which are commonly lethal by 13.5 d.p.c., was disrupted due to apoptosis of the metanephric mesenchyme and a failure of ureteric bud branching (35). Subsequent *in vitro* organ culture experiments and transgenic animal studies proved a requirement of Wt1 not only for the early inductive events but also during the later phases of kidney formation (*i.e.* the differentiation and maturation of the glomeruli) (46) and for the integrity of mature kidneys (47–49). Interestingly, recent disruption of the *Adamts16* gene in Dahl Salt-sensitive rats caused splitting and thickening of glomerular capillaries in addition to a significant reduction of arterial blood pressure (50). Renal damage was associated with increased proteinuria, suggesting that Adamts16 is indeed necessary for the structural and functional preservation of the kidneys in this model of genetic hypertension (50).

Interaction of the Wt1 transcription factor with the *Adamts16* gene may also play a role in the development and function of the gonads. The mammalian gonads are formed by tissue that is derived from the intermediate mesoderm on either side of the embryonic midline axis (51). Establishment of the bipotential gonadal ridge occurs in a non-sex-specific manner in XX and XY individuals and is completed by ~12 d.p.c. in rats and mice (51). Wt1 acts on multiple steps during gonad development. Gonadal ridge formation in *Wt1* null mice is initiated in both males and females but then degenerates due to apoptosis, leading to gonadal agenesis (35). The sex-determining factor Sry and the anti-Müllerian hormone receptor (Amhr) 2, which is critical for the regression of the female urogenital

ducts, are among the genes that are regulated by Wt1 (41, 52, 53). Consistently, male-to-female sex reversal or genital tract abnormalities were observed in XY patients with heterozygous *Wt1* germ line mutations (54), underscoring the role of Wt1 in testis determination. Our results indicate that Wt1 controls *Adamts16* expression in the developing gonads in a time-dependent and sex-specific fashion. Thus, silencing of *Wt1* significantly increased *Adamts16* transcripts in *in vitro* cultured XY gonads of 11.5 and 12.5 d.p.c. embryos (Fig. 3*C*). In contrast, *Adamts16* mRNA levels in female but not in male gonads (12.5 and 13.5 d.p.c.) were significantly reduced by *Wt1* antisense inhibition (Fig. 3, *C* and *D*). These results suggest that Wt1 inhibits *Adamts16* expression in XY gonads during the early developmental stages and stimulates *Adamts16* expression in XX gonads at later points in time. Repression of Adamts16 by Wt1 in developing XY gonads is in line with our failure to clearly co-localize both proteins in the same cells in this tissue (Fig. 1, *A* and *B*). Further on, Wt1 may directly contribute to the developmental increase of *Adamts16* mRNA levels in female gonads (Fig. 3*B*). Reporter gene assays and protein-DNA binding studies confirmed that Wt1(−KTS) protein indeed stimulates transcription of the *Adamts16* gene in ovarian granulosa cells (Figs. 6 and 7). The molecular mechanisms underlying the variable stage-specific effects of Wt1 on *Adamts16* expression in male and female gonads are currently unknown but may involve the physical interaction of Wt1 with other proteins in the control of gene transcription (55). Detection of Adamts16 in spermatids of mature testes (Fig. 1, *A* and *C*) points to a role in male germ cell maturation and/or function throughout adulthood. Generation of mouse mutants with conditional inactivation of the *Adamts16* gene in the gonads will be helpful in clarifying this issue.

It has been shown previously that FSH induced the expression of ADAMTS16 in parietal granulosa cells of preovulatory human follicles (16). In contrast, FSH attenuated basal and nerve growth factor-stimulated Wt1 protein expression in isolated granulosa cells of 21-day-old mice (56). Recently, Wt1 has been reported to inhibit expression of the FSH receptor in immature rat granulosa cells through repression of the FSH receptor promoter (57). These combined observations suggest that Wt1 is an important element in the hormonally regulated transcriptional network in preovulatory follicles. Stimulation of *Adamts16* expression by Wt1 in parietal granulosa cells may have a role in extracellular matrix (ECM) remodeling, which is a prerequisite for oocyte liberation during ovulation. Notably, various members of the ADAMTS protease family, in particular ADAMTS1, have been implicated in ECM transformation in the ovary (44, 58–60). The involvement of other proteases and substrates in this process adds some functional redundancy, which may facilitate ovulation even in the absence of one or more constituents (61).

Another interesting aspect of our study pertains to the presumed origin of the follicular granulosa cells, which is still a matter of controversy. Indeed, three major sources for pregranulosa cells have been under discussion for many decades: 1) mesothelial cells on the surface of the developing ovary (62), 2) cells originating from a centrally located blastema (63), and 3) mesonephric cells derived from the rete ovarii system (64). The results of a more recent histological study in sheep favored the idea that >95% of the granulosa cells in newly formed primordial follicles arise from the ovarian surface epithelium (65). During this process, mesothelial cells on the outside of the ovary are expected to undergo epithelial-to-mesenchymal transition and migrate into the ovarian cortex, where they differentiate to follicular granulosa cells. Remarkably, Wt1 protein has been identified to act as a key molecule for epithelial-to-mesenchymal transition by down-regulating E-cadherin expression in the epicardium of mouse embryos and other mesothelial tissues (66). Thus, co-localization with Wt1 protein in the ovarian surface epithelium suggests that Adamts16 promotes a mesenchymal commitment of these cells, possibly through ECM remodeling.

In summary, our findings demonstrate that transcription of the gene encoding the Adamts16 metalloproteinase is regulated by the Wilms tumor protein Wt1 in a sex- and tissue-specific fashion. This regulatory link has a presumed role in the development of murine kidneys and gonads.

Acknowledgment—We thank Ulrike Neumann for expert technical assistance.

REFERENCES

1. Cal, S., Obaya, A. J., Llamazares, M., Garabaya, C., Quesada, V., and López-Otin, C. (2002) Cloning, expression analysis, and structural characterization of seven novel human ADAMTSs, a family of metalloproteinases with disintegrin and thrombospondin-1 domains. *Gene* **283,** 49–62
2. Apte, S. S. (2009) A disintegrin-like and metalloprotease (reprolysin-type) with thrombospondin type 1 motif (ADAMTS) superfamily. Functions and mechanisms. *J. Biol. Chem.* **284,** 31493–31497
3. Kuno, K., and Matsushima, K. (1998) ADAMTS-1 protein anchors at the extracellular matrix through the thrombospondin type I motifs and its spacing region. *J. Biol. Chem.* **273,** 13912–13917
4. Kuno, K., Kanada, N., Nakashima, E., Fujiki, F., Ichimura, F., and Matsushima, K. (1997) Molecular cloning of a gene encoding a new type of metalloproteinase-disintegrin family protein with thrombospondin motifs as an inflammation associated gene. *J. Biol. Chem.* **272,** 556–562
5. Colige, A., Beschin, A., Samyn, B., Goebels, Y., Van Beeumen, J., Nusgens, B. V., and Lapière, C. M. (1995) Characterization and partial amino acid sequencing of a 107-kDa procollagen I N-proteinase purified by affinity chromatography on immobilized type XIV collagen. *J. Biol. Chem.* **270,** 16724–16730
6. Fernandes, R. J., Hirohata, S., Engle, J. M., Colige, A., Cohn, D. H., Eyre, D. R., and Apte, S. S. (2001) Procollagen II amino propeptide processing by ADAMTS-3. Insights on dermatosparaxis. *J. Biol. Chem.* **276,** 31502–31509
7. Tortorella, M. D., Burn, T. C., Pratta, M. A., Abbaszade, I., Hollis, J. M., Liu, R., Rosenfeld, S. A., Copeland, R. A., Decicco, C. P., Wynn, R., Rockwell, A., Yang, F., Duke, J. L., Solomon, K., George, H., Bruckner, R., Nagase, H., Itoh, Y., Ellis, D. M., Ross, H., Wiswall, B. H., Murphy, K., Hillman, M. C., Jr., Hollis, G. F., Newton, R. C., Magolda, R. L., Trzaskos, J. M., and Arner, E. C. (1999) Purification and cloning of aggrecanase-1. A member of the ADAMTS family of proteins. *Science* **284,** 1664–1666
8. Vázquez, F., Hastings, G., Ortega, M. A., Lane, T. F., Oikemus, S., Lombardo, M., and Iruela-Arispe, M. L. (1999) METH-1, a human ortholog of ADAMTS-1, and METH-2 are members of a new family of proteins with angio-inhibitory activity. *J. Biol. Chem.* **274,** 23349–23357
9. Clark, M. E., Kelner, G. S., Turbeville, L. A., Boyer, A., Arden, K. C., and Maki, R. A. (2000) ADAMTS9, a novel member of the ADAM-TS/metallospondin gene family. *Genomics* **67,** 343–350
10. Hurskainen, T. L., Hirohata, S., Seldin, M. F., and Apte, S. S. (1999) ADAM-TS5, ADAM-TS6, and ADAM-TS7, novel members of a new family

of zinc metalloproteinases. General features and genomic distribution of the ADAM-TS family. *J. Biol. Chem.* **274,** 25555–25563
11. Kim, J., Kim, H., Lee, S. J., Choi, Y. M., Lee, S. J., and Lee, J. Y. (2005) Abundance of ADAM-8, -9, -10, -12, -15 and -17 and ADAMTS-1 in mouse uterus during the oestrous cycle. *Reprod. Fertil. Dev.* **17,** 543–555
12. Sylvester, J., Liacini, A., Li, W. Q., and Zafarullah, M. (2004) Interleukin-17 signal transduction pathway implicated in inducing matrix metalloproteinase-3, -13 and aggrecanase-1 genes in articular chondrocytes. *Cell. Signal.* **16,** 469–476
13. Worley, J. R., Baugh, M. D., Hughes, D. A., Edwards, D. R., Hogan, A., Sampson, M. J., and Gavrilovic, J. (2003) Metalloproteinase expression in PMA-stimulated THP-1 cells. Effects of peroxisome proliferator-activated receptor-γ (PPR γ) agonists and 9-*cis*-retinoic acid. *J. Biol. Chem.* **278,** 51340–51346
14. Colige, A., Nuytinck, L., Hausser, I., van Essen, A. J., Thiry, M., Herens, C., Adès, L. C., Malfait, F., Paepe, A. D., Franck, P., Wolff, G., Oosterwijk, J. C., Smitt, J. H., Lapière, C. M., and Nusgens, B. V. (2004) Novel types of mutation responsible for the dermatosparactic type of Ehlers-Danlos syndrome (Type VIIC) and common polymorphisms in the ADAMTS2 gene. *J. Invest. Dermatol.* **123,** 656–663
15. Levy, G. G., Nichols, W. C., Lian, E. C., Foroud, T., McClintick, J. N., McGee, B. M., Yang, A. Y., Siemieniak, D. R., Stark, K. R., Gruppo, R., Sarode, R., Shurin, S. B., Chandrasekaran, V., Stabler, S. P., Sabio, H., Bouhassira, E. E., Upshaw, J. D., Jr., Ginsburg, D., and Tsai, H. M. (2001) Mutations in a member of the ADAMTS gene family cause thrombotic thrombocytopenic purpura. *Nature* **413,** 488–494
16. Gao, S., De Geyter, C., Kossowska, K., and Zhang, H. (2007) FSH stimulates the expression of the ADAMTS-16 protease in mature human ovarian follicles. *Mol. Hum. Reprod.* **13,** 465–471
17. Kevorkian, L., Young, D. A., Darrah, C., Donell, S. T., Shepstone, L., Porter, S., Brockbank, S. M., Edwards, D. R., Parker, A. E., and Clark, I. M. (2004) Expression profiling of metalloproteinases and their inhibitors in cartilage. *Arthritis Rheum.* **50,** 131–141
18. Joe, B., Saad, Y., Dhindaw, S., Lee, N. H., Frank, B. C., Achinike, O. H., Luu, T. V., Gopalakrishnan, K., Toland, E. J., Farms, P., Yerga-Woolwine, S., Manickavasagam, E., Rapp, J. P., Garrett, M. R., Coe, D., Apte, S. S., Rankinen, T., Pérusse, L., Ehret, G. B., Ganesh, S. K., Cooper, R. S., O'Connor, A., Rice, T., Weder, A. B., Chakravarti, A., Rao, D. C., and Bouchard, C. (2009) Positional identification of variants of *Adamts16* linked to inherited hypertension. *Hum. Mol. Genet.* **18,** 2825–2838
19. Sakamoto, N., Oue, N., Noguchi, T., Sentani, K., Anami, K., Sanada, Y., Yoshida, K., and Yasui, W. (2010) Serial analysis of gene expression of esophageal squamous cell carcinoma. ADAMTS16 is upregulated in esophageal squamous cell carcinoma. *Cancer Sci.* **101,** 1038–1044
20. Surridge, A. K., Rodgers, U. R., Swingler, T. E., Davidson, R. K., Kevorkian, L., Norton, R., Waters, J. G., Goldring, M. B., Parker, A. E., and Clark, I. M. (2009) Characterization and regulation of ADAMTS-16. *Matrix Biol.* **28,** 416–424
21. Larsson, S. H., Charlieu, J. P., Miyagawa, K., Engelkamp, D., Rassoulzadegan, M., Ross, A., Cuzin, F., van Heyningen, V., and Hastie, N. D. (1995) Subnuclear localization of WT1 in splicing or transcription factor domains is regulated by alternative splicing. *Cell* **81,** 391–401
22. Sciesielski, L. K., Kirschner, K. M., Scholz, H., and Persson, A. B. (2010) Wilms' tumor protein Wt1 regulates the interleukin-10 (IL-10) gene. *FEBS Lett.* **584,** 4665–4671
23. Englert, C., Hou, X., Maheswaran, S., Bennett, P., Ngwu, C., Re, G. G., Garvin, A. J., Rosner, M. R., and Haber, D. A. (1995) WT1 suppresses synthesis of the epidermal growth factor receptor and induces apoptosis. *EMBO J.* **14,** 4662–4675
24. Hartwig, S., Ho, J., Pandey, P., Macisaac, K., Taglienti, M., Xiang, M., Alterovitz, G., Ramoni, M., Fraenkel, E., and Kreidberg, J. A. (2010) Genomic characterization of Wilms' tumor suppressor 1 targets in nephron progenitor cells during kidney development. *Development* **137,** 1189–1203
25. Clapcote, S. J., and Roder, J. C. (2005) Simplex PCR assay for sex determination in mice. *BioTechniques* **38,** 702
26. Dame, C., Kirschner, K. M., Bartz, K. V., Wallach, T., Hussels, C. S., and Scholz, H. (2006) Wilms' tumor suppressor, Wt1, is a transcriptional activator of the erythropoietin gene. *Blood* **107,** 4282–4290
27. Kirschner, K. M., Hagen, P., Hussels, C. S., Ballmaier, M., Scholz, H., and Dame, C. (2008) The Wilms' tumor suppressor Wt1 activates transcription of the erythropoietin receptor in hematopoietic progenitor cells. *FASEB J.* **22,** 2690–2701
28. Martens, L. K., Kirschner, K. M., Warnecke, C., and Scholz, H. (2007) Hypoxia-inducible factor-1 (HIF-1) is a transcriptional activator of the TrkB neurotrophin receptor gene. *J. Biol. Chem.* **282,** 14379–14388
29. Warburg, O., and Christian, W. (1942) Isolation and crystallization of enolase. *Biochem. Z.* **310,** 384–421
30. Wagner, K. D., Wagner, N., Sukhatme, V. P., and Scholz, H. (2001) Activation of vitamin D receptor by the Wilms' tumor gene product mediates apopotsis of renal cells. *J. Am. Soc. Nephrol.* **12,** 1188–1196
31. Wagner, N., Wagner, K. D., Theres, H., Englert, C., Schedl, A., and Scholz, H. (2005) Coronary vessel development requires activation of the TrkB neurotrophin receptor by the Wilms' tumor transcription factor Wt1. *Genes Dev.* **19,** 2631–2642
32. Stricker, S., Verhey van Wijk, N., Witte, F., Brieske, N., Seidel, K., and Mundlos, S. (2006) Cloning and expression pattern of chicken Ror2 and functional characterization of truncating mutations in Brachydactyly type B and Robinow syndrome. *Dev. Dyn.* **235,** 3456–3465
33. Pritchard-Jones, K., Fleming, S., Davidson, D., Bickmore, W., Porteous, D., Gosden, C., Bard, J., Buckler, A., Pelletier, J., and Housman, D. (1990) The candidate Wilms' tumour gene is involved in genitourinary development. *Nature* **346,** 194–197
34. Armstrong, J. F., Pritchard-Jones, K., Bickmore, W. A., Hastie, N. D., and Bard, J. B. (1993) The expression of the Wilms' tumour gene, WT1, in the developing mammalian embryo. *Mech. Dev.* **40,** 85–97
35. Kreidberg, J. A., Sariola, H., Loring, J. M., Maeda, M., Pelletier, J., Housman, D., and Jaenisch, R. (1993) WT-1 is required for early kidney development. *Cell* **74,** 679–691
36. Haber, D. A., Sohn, R. L., Buckler, A. J., Pelletier, J., Call, K. M., and Housman, D. E. (1991) Alternative splicing and genomic structure of the Wilms' tumor gene WT1. *Proc. Natl. Acad. Sci. U.S.A.* **88,** 9618–9622
37. Madden, S. L., Cook, D. M., Morris, J. F., Gashler, A., Sukhatme, V. P., and Rauscher, F. J., 3rd (1991) Transcriptional repression mediated by the WT1 Wilms tumor gene product. *Science* **253,** 1550–1553
38. Hamilton, T. B., Barilla, K. C., and Romaniuk, P. J. (1995) High affinity binding sites for the Wilms' tumour suppressor protein WT1. *Nucleic Acids Res.* **23,** 277–284
39. Laity, J. H., Dyson, H. J., and Wright, P. E. (2000) Molecular basis for modulation of biological function by alternate splicing of the Wilms' tumor suppressor protein. *Proc. Natl. Acad. Sci. U.S.A.* **97,** 11932–11935
40. Bor, Y. C., Swartz, J., Morrison, A., Rekosh, D., Ladomery, M., and Hammarskjöld, M. L. (2006) The Wilms' tumor 1 (WT1) gene (+KTS isoform) functions with a CTE to enhance translation from an unspliced RNA with a retained intron. *Genes Dev.* **20,** 1597–1608
41. Klattig, J., Sierig, R., Kruspe, D., Besenbeck, B., and Englert, C. (2007) The Wilms' tumor protein Wt1 is an activator of the anti-Müllerian hormone receptor gene Amhr2. *Mol. Cell. Biol.* **27,** 4355–4364
42. Michos, O. (2009) Kidney development. From ureteric bud formation to branching morphogenesis. *Curr. Opin. Genet. Dev.* **19,** 484–490
43. Pohl, M., Sakurai, H., Bush, K. T., and Nigam, S. K. (2000) Matrix metalloproteinases and their inhibitors regulate *in vitro* ureteric bud branching morphogenesis. *Am. J. Physiol. Renal Physiol.* **279,** F891–F900
44. Mittaz, L., Russell, D. L., Wilson, T., Brasted, M., Tkalcevic, J., Salamonsen, L. A., Hertzog, P. J., and Pritchard, M. A. (2004) Adamts-1 is essential for the development and function of the urogenital system. *Biol. Reprod.* **70,** 1096–1105
45. Miller-Hodges, E., and Hohenstein, P. (2012) WT1 in disease. Shifting the epithelial-mesenchymal balance. *J. Pathol.* **226,** 229–240
46. Davies, J. A., Ladomery, M., Hohenstein, P., Michael, L., Shafe, A., Spraggon, L., and Hastie, N. (2004) Development of an siRNA-based method for repressing specific genes in renal organ culture and its use to show that the Wt1 tumour suppressor is required for nephron differentiation. *Hum. Mol. Genet.* **13,** 235–246
47. Guo, J. K., Menke, A. L., Gubler, M. C., Clarke, A. R., Harrison, D., Hammes, A., Hastie, N. D., and Schedl A. (2002) WT1 is a key regulator of

podocyte function. Reduced expression levels cause crescentic glomerulonephritis and mesangial sclerosis. *Hum. Mol. Genet.* **11,** 651–659
48. Schumacher, V., Schärer, K., Wühl, E., Altrogge, H., Bonzel, K. E., Guschmann, M., Neuhaus, T. J., Pollastro, R. M., Kuwertz-Bröking, E., Bulla, M., Tondera, A. M., Mundel, P., Helmchen, U., Waldherr, R., Weirich, A., and Royer-Pokora, B. (1998) Spectrum of early onset nephrotic syndrome associated with WT1 missense mutations. *Kidney Int.* **53,** 1594–1600
49. Niaudet, P., and Gubler, M. C. (2006) WT1 and glomerular diseases. *Pediatr. Nephrol.* **21,** 1653–1660
50. Gopalakrishnan, K., Kumarasamy, S., Abdul-Majeed, S., Kalinoski, A. L., Morgan, E. E., Gohara, A. F., Nauli, S. M., Filipiak, W. E., Saunders, T. L., and Joe, B. (2012) Targeted disruption of *Adamts16* gene in a rat genetic model of hypertension. *Proc. Natl. Acad. Sci. U.S.A.* **109,** 20555–20559
51. Swain, A., and Lovell-Badge, R. (1999) Mammalian sex differentiation: a molecular drama. *Genes Dev.* **13,** 755–767
52. Shimamura, R., Fraizer, G. C., Trapman, J., Lau, Y.-f. C., and Saunders, G. F. (1997) The Wilms' tumor gene WT1 can regulate genes involved in sex determination and differentiation SRY, Müllerian-inhibiting substance, and the androgen receptor. *Clin. Cancer Res.* **3,** 2571–2580
53. Hossain, A., and Saunders, G. F. (2001) The human sex-determining gene SRY is a direct target of WT1. *J. Biol. Chem.* **276,** 16817–16823
54. Pelletier, J., Bruening, W., Kashtan, C. E., Mauer, S. M., Manivel, J. C., Striegel, J. E., Houghton, D. C., Junien, C., Habib, R., and Fouser, L. (1991) Germline mutation in the Wilms' tumor suppressor gene are associated with abnormal urogenital development and Denys-Drash syndrome. *Cell* **67,** 437–447
55. Roberts, S. G. (2006) The modulation of WT1 transcription function by cofactors. *Biochem. Soc. Symp.* **73,** 191–201
56. Roh, J., Bae, J., Lee, K., Mayo, K., Shea, L., and Woodruff, T. K. (2009) Regulation of Wilms' tumor gene expression by nerve growth factor and follicle-stimulating hormone in the immature mouse ovary. *Fertil. Steril.* **91,** 1451–1454
57. Yoon, O., and Roh, J. (2012) Regulation of FSH receptor expression by the Wilms' tumor 1 gene product (WT1) in immature rat granulosa cells. *Mol. Reprod. Dev.* **79,** 368
58. Espey, L. L., Yoshioka, S., Russell, D. L., Robker, R. L., Fujii, S., and Richards, J. S. (2000) Ovarian expression of a disintegrin and metalloproteinase with thrombospondin motifs during ovulation in the gonadotropin-primed immature rat. *Biol. Reprod.* **62,** 1090–1095
59. Madan, P., Bridges, P. J., Komar, C. M., Beristain, A. G., Rajamahendran, R., Fortune, J. E., and MacCalman, C. D. (2003) Expression of messenger RNA for ADAMTS subtypes changes in the periovulatory follicle after the gonadotropin surge and during luteal development and regression in cattle. *Biol. Reprod.* **69,** 1506–1514
60. Robker, R. L., Russell, D. L., Espey, L. L., Lydon, J. P., O'Malley, B. W., and Richards, J. S. (2000) Progesteron-regulated genes in the ovulation process. ADAMTS-1 and cathepsin L proteases. *Proc. Natl. Acad. Sci. U.S.A.* **97,** 4689–4694
61. Richards, J. S., Hernandez-Gonzalez, I., Gonzalez-Robayna, I., Teuling, E., Lo, Y., Boerboom, D., Falender, A. E., Doyle, K. H., LeBaron, R. G., Thompson, V., and Sandy, J. D. (2005) Regulated expression of ADAMTS family members in follicles and cumulus oocyte complexes. Evidence for specific and redundant patterns during ovulation. *Biol. Reprod.* **72,** 1241–1255
62. Gondos, B. (1975) Surface epithelium of the developing ovary. Possible correlation with ovarian neoplasia. *Am. J. Pathol.* **81,** 303–321
63. Peters, H., and Pedersen, T. (1967) Origin of follicle cells in the infant mouse ovary. *Fertil. Steril.* **18,** 309–313
64. Byskov, A. G. (1978) The anatomy and ultrastructure of the rete system in the fetal mouse ovary. *Biol. Reprod.* **19,** 720–735
65. Sawyer, H. R., Smith, P., Heath, D. A., Juengel, J. L., Wakefield, S. J., and McNatty, K. P. (2002) formation of ovarian follicles during fetal development in sheep. *Biol. Reprod.* **66,** 1134–1150
66. Martínez-Estrada, O. M., Lettice, L. A., Essafi, A., Guadix, J. A., Slight, J., Velecela, V., Hall, E., Reichmann, J., Devenney, P. S., Hohenstein, P., Hosen, N., Hill, R. E., Muñoz-Chapuli, R., and Hastie, N. D. (2010) Wt1 is required for cardiovascular progenitor cell formation through transcriptional control of Snail and E-cadherin. *Nat. Genet.* **42,** 89–93
67. Morris, J. F., Madden, S. L., Tournay, O. E., Cook, D. M., Sukhatme, V. P., and Rauscher, F. J. (1991) Characterization of the zinc finger protein encoded by the WT1 Wilms' tumor locus. *Oncogene* **6,** 2339–2348